Organic

By Brylee David B. Tiu, Sicily B. Tiu, Jennifer R. Wang, and Prof. R.C. Advincula, Case Western Reserve University; Simonida Grubjesic, Anthony F. Toussaint, Nathan Kofira, and Tony Gichuhi, ICL | Advanced Additives

Improved Corrosion Protection Due to

Corrosion Inhibitors in Waterborne Paint Coatings

The cost of corrosion is one of the biggest economic challenges in a number of industries worldwide. Although complete eradication of corrosion is impossible, significant reduction in the corrosion rate can be achieved using various corrosion mitigation techniques, most notably using protective polymeric coatings. In this regard, the eco-friendly properties of waterborne paints have been attracting widespread attention in recent years due to the promulgation of lower allowable volatile organic compound content. However, these coatings are prone to increased penetration of moisture and corrosive species. To improve the protective properties of the coating, we incorporated two non–toxic organic corrosion additives into a waterborne acrylic paint formulation and evaluated their anticorrosion properties using a combination of electrochemical tests, microscopy, and spectroscopic techniques.

INTRODUCTION

Defined as the inevitable degradation of metals in various environments, corrosion is an enormous economic and technical problem that has constantly plagued various industrial sectors worldwide. As mandated by the U.S. Congress, initiated by the National Association of Corrosion Engineers (NACE) International, and conducted by CC Technologies Laboratories, Inc., a U.S. Federal Highway Administration (FHWA) study estimated the direct costs of corrosion in every U.S.-based industry sector from 1999–2001. Based on the results of the study, the annual corrosion costs total U.S.$ 276 billion, which is almost 3.1% of the country's Gross Domestic Product (GDP).[1] A huge portion of this cost that amounts to U.S.$ 121 billion (1.4% of the U.S. GDP) is attributed to various corrosion mitigation techniques; 88.3% is allotted for organic corrosion protective coatings.[1] In March 2016, NACE International released the report, entitled "IMPACT—the International Measures of Prevention, Application, and Economics of Corrosion Technologies," wherein the global cost of corrosion was estimated to reach U.S.$ 2.5 trillion or approximately 3.4% of the global GDP.[2] The study also claims that between 15–35% of this total cost (equivalent to U.S.$ 375–875 billion) can potentially be saved if existing corrosion control measures are properly executed and incorporated into existing industries.

Organic Corrosion Inhibitors in Waterborne Paint Coatings

It is widely accepted that absolute corrosion mitigation is impossible; however, various protocols can be used to significantly slow down the rate of corrosion. The most common of these techniques is the application of protective coatings, in which corrosion-inhibiting additives can be applied onto metal surfaces. In particular, the more environmentally friendly waterborne paints are becoming much more attractive as compared to the solventborne systems due to the increasingly stringent regulations for the incorporation of volatile organic compounds (VOC).[3] In terms of corrosion resistance, most waterborne coatings are more prone to water and electrolyte penetration, which results in poorer anticorrosive performance of the paint film. Under corrosive conditions, these coatings can exhibit blistering, anodic undermining, and delamination.[3] To address these issues, corrosion inhibitive pigments and additives are incorporated into these coatings to promote better adhesion to the metal surface or impede either the cathodic or anodic corrosive reactions.[4] Traditional additives may contain chromate or lead-based materials; however, other less toxic nonchromate based inorganic inhibitors such as silicates, phosphates, borates, and vanadates are becoming more common. Furthermore, the use of the organic corrosion inhibitors has gained much popularity in recent years. There is a growing trend of combining them with inorganic pigments to obtain optimal coating performance. Most organic corrosion inhibitors are considered environmentally friendly as these chemicals present a viable alternative to existing inorganic corrosion inhibitors. Organic corrosion inhibitors can be used alone or in combination with inorganic corrosion inhibitors, providing dual protective modes of action, and thus enhancing the anticorrosive properties of a coating. While, on one hand, these materials can protect metal substrates through anodic or cathodic passivation mechanisms similar to inorganic inhibitors, organic corrosion inhibitors also have unique capabilities to enhance barrier properties, promote adhesion, and improve substrate wetting due to their intrinsic hydrophobic nature. Organic corrosion inhibitors are used at significantly lower loading levels compared to inorganic corrosion inhibitors and, in some cases, optimized coating performance and cost savings is achieved as a result of this reduction in corrosion inhibitive demand. In addition, benefits specific to the ease of use by paint formulators is attributed to the organic corrosion inhibitors, since they can often be post-added to the paint formulation in a liquid form.

In this work, we demonstrate the improvements in the corrosion inhibiting properties of an acrylic waterborne paint using two commercially available nontoxic organic corrosion inhibitors. The H570 inhibitor is an organic acid-amine complex, while the H650 additive is an organic di-acid. The corrosion protective behavior was evaluated against an aqueous solution containing 5% NaCl using electrochemical measurements, and spectroscopic and microscopic surface imaging techniques. Electrochemical corrosion testing provides fast information about the degradation of the coatings and the ongoing corrosion events without any visible corrosion induced damages. These results were correlated with the immersion test results to accurately gauge improvements to corrosion inhibition due to the incorporation of organic corrosion inhibitive additives.

TABLE 1—Individual Components of the Control Water-based Paint Formulation

INGREDIENTS AND INSTRUCTIONS	Wt (g)	Wt%	Vol %
JONCRYL 1522	631.9	60.20	79.51
DOWANOL DPNP	42.7	4.07	6.17
DISPERBYK-2012	20.5	1.95	2.58
TEGO 901W	11.67	1.11	0
SURFYNOL 104DPM	2.5	0.24	0.36
8001 RUTILE TITANIUM DIOXIDE	172.66	16.4	5.46
BAYFERROX 318NM	14.3	1.36	0.41
ZEEOSPHERES G-400	24.35	2.32	1.35
MICRO TALC IT EXTRA	75.05	7.15	3.56
FLASH X-150	5.25	0.50	0
BYK-348	4.75	0.45	0.6
WATER	44.12	4.20	0
TOTAL	**1049.75**	**100**	**100**

EXPERIMENTAL

Corrosion-resistant Paint Formulation and Sample Preparation

For all electrochemical corrosion tests, the substrate used was a 1/16 in. thick impact resistant A516 carbon steel [Item #1631T11, purchased from McMaster-Carr (Aurora, OH)]. The substrate was cut into 1.5 cm × 2 cm coupons using a vertical band saw (Model V-20, Wellsaw, Kalamazoo, MI) with a medium (10–14 TPI) blade. Prior to application of the acrylic waterborne paint, the carbon steel substrates were polished with emery papers of increasing grit (60, 220, 400, 600, and 1000), thoroughly rinsed in acetone, dried with N_2, and stored in a vacuum desiccator for at least one hour.

The acrylic waterborne paint formulation was provided by ICL\ Advanced Additives, USA. *Table 1* lists all the ingredients and corresponding composition of the paint formulation. Meanwhile, *Table 2* presents the key physical properties of the resulting mixture. Corrosion inhibitors, which will be denoted as H570 and H650, respectively, were also sourced from ICL\ Advanced Additives, USA. Since these inhibitors were initially in powder form, pre-neutralized aqueous solutions in water were prepared prior to mixing with the paint. The inhibitor solutions were prepared by mixing 3 g of additive into a solution containing

TABLE 2—Physical Properties of the Control Water-based Paint in the Study

PROPERTY	VALUE
DENSITY (LB/GAL)	11.64
DENSITY (G/L)	1394.65
WEIGHT PIGMENT (%)	25.92
VOLUME PIGMENT (%)	10.37
WEIGHT SOLIDS (%)	54.97
VOLUME SOLIDS (%)	48.42
PIGMENT VOLUME CONCENTRATION (%)	21.94
VOC (LB/GAL)	0.85
VOC (G/L)	102.34

0.8 mL of ammonium hydroxide and 6.28 mL of MilliQ water. Afterwards, paint formulations containing various concentrations of the two organic corrosion inhibitors were prepared using an overhead mixer by post-adding the aqueous liquid organic corrosion inhibitor solutions. The prepared carbon steel substrates were then immersed into the paint vertically. Using a dip coater, the carbon steel samples were lifted from the paint at a controlled rate of 25 mm/min and allowed to cure for seven days prior to corrosion testing. The dry film thicknesses of all applied coatings ranged from 25–35 μm, as measured using a P-6 stylus profilometer, KLA-Tencor (Milpitas, CA). The profiler was set to run at 100 μm/sec with a sampling rate of 200 Hz, applied force of 2 mg, and scan length of 2023 μm.

Electrochemical Corrosion Testing

The coated carbon steel sample was incorporated into a standard three-electrode cell for the electrochemical corrosion testing in 5% aqueous NaCl solution, as shown in *Figure 1*. A Teflon chamber with a cylindrical hole in the middle was clamped onto the steel with a Viton O-ring in between to prevent leaks. The use of the chamber ensured that a constant area of 0.785 cm^2 is exposed to the electrolyte. An aqueous Ag/AgCl electrode and platinum wire were used as the reference and counter electrodes respectively. The setup was then connected to an Autolab PGSTAT 12 potentiostat (MetroOhm, USA), which was controlled by the GPES (Ver. 4.9) and Frequency Response Analyzer (FRA) programs.

The coated samples were then exposed to 5% aqueous NaCl solution, while the open-circuit potential (E_{OCP}) was being recorded. After one hour, electrochemical impedance spectroscopy (EIS) data was measured at 50 different frequencies from 100 kHz to 10 mHz as an AC voltage signal with an amplitude voltage of 10 mV was applied. The impedance spectra were fitted to equivalent circuit models using the EIS Spectrum Analyser software (ABC-Chemistry.org) according to the Powell algorithm.

Surface Morphology

The surface morphology of the uncoated and paint-coated carbon steel samples was characterized using tapping mode atomic force microscopy (AFM). AFM measurements were conducted using a PicoScan 2500 AFM (Agilent Technologies) with a piezo scanner that was set to scan the films at 1–1.5 lines/sec. Commercially available tapping mode cantilevers (NSG30, single crystal silicon, NT-MDT) with a resonant frequency in the range of 240–440 kHz were employed. The Gwyddion Software (Ver. 2.19) was used to filter and analyze all AFM micrographs. Meanwhile, a JEOL scanning electron microscope (JEOL-JSM-6510LV) was used to image the resulting surface morphologies of the uncoated and coated samples after immersion in 5% NaCl for 24 h. The SEM micrographs were recorded with an acceleration voltage 30 kV and working distance of 14 mm.

Attenuated Total Reflectance-Infrared (ATR-IR) and Raman Spectroscopy

After immersing in 5% NaCl for three weeks, the infrared spectra of the uncoated and coated samples were analyzed in attenuated total reflectance (ATR) mode using the Cary 680 FTIR spectrometer from Agilent Technologies (Santa Clara, CA) with the GladiATR accessory from Pike Technologies (Fitchburg, WI). On the other hand, the I-Raman Plus from BWTek (Newark, DE) was used to collect the Raman spectra of the samples using a 100% laser power and 30-sec integration time.

FIGURE 1—Standard three-electrode electrochemical cell for corrosion testing.

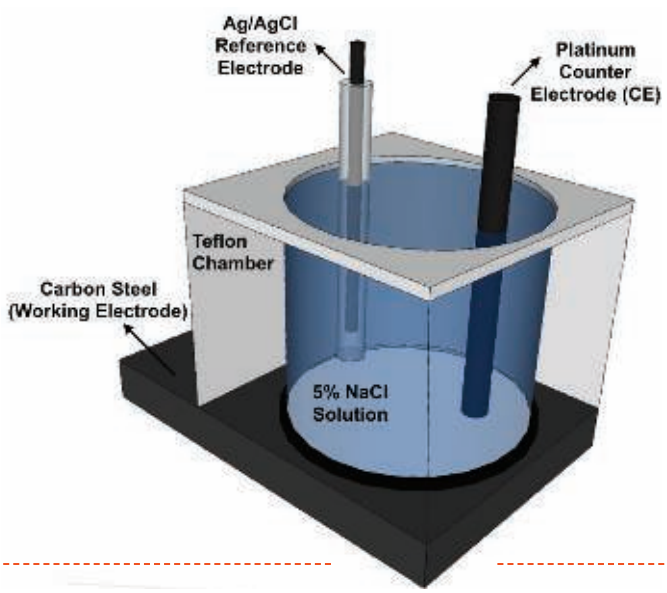

RESULTS AND DISCUSSION

Open-Circuit Potential Measurements

The E_{OCP} measurements were first used to evaluate the anticorrosive properties of the coating. The E_{OCP} is known as the potential difference between the carbon steel surface (working electrode) and the Ag/AgCl reference electrode without any application of a potential or a current. It provides information on the corrosion behavior of the system based on the steady-state corrosion potential recorded. The decrease in the E_{OCP} value indicates the spontaneous oxidation and dissolution of the metal substrate due to exposure to the corrosive environment. Alternatively, the increase in the E_{OCP} value indicates the formation of the corrosion products and/or passive film, which can decrease the corrosion rate.

Figure 2 presents the E_{OCP} measurements of the bare (uncoated) and coated carbon steel (CS) samples in 5% aqueous NaCl solution as a function of immersion time. For the bare substrate, the E_{OCP} decreased sharply from –0.481 V,

FIGURE 2—Open circuit potential (E_{OCP}) measurements of the bare and coated carbon steel samples in 5% NaCl.

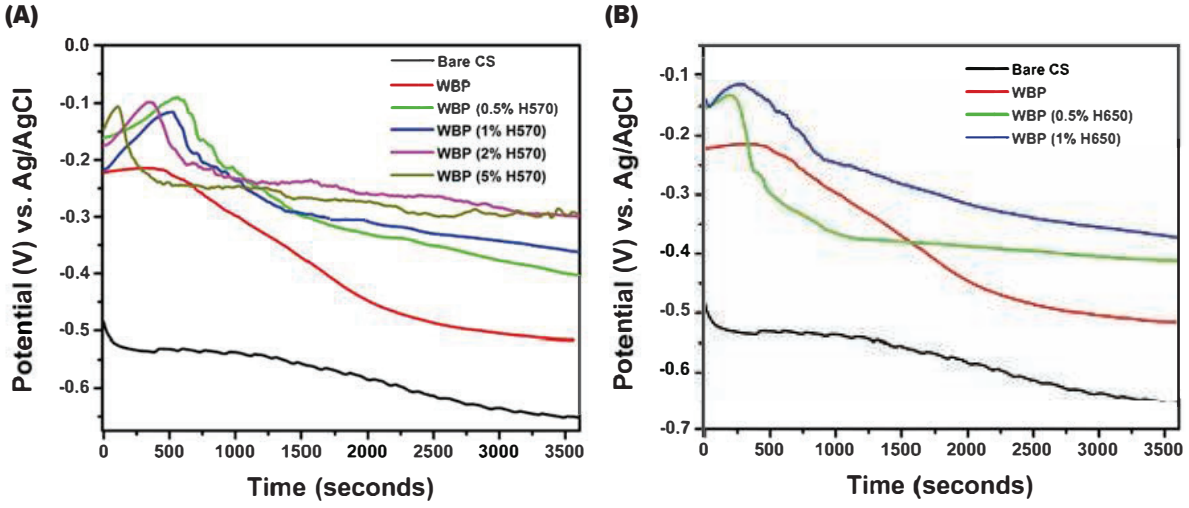

FIGURE 3—(A) Nyquist and (B) Bode impedance plots of the bare and H570-paint coated carbon steel samples after immersion in the 5% aqueous NaCl solution for one hour.

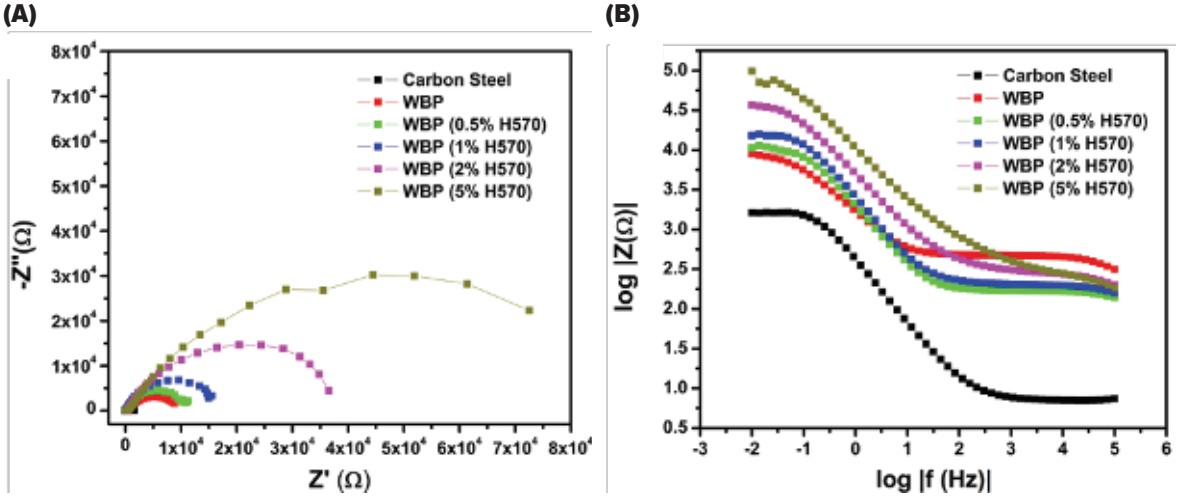

FIGURE 4—Equivalent circuit models for the (A) bare carbon steel and (B) paint-coated substrates.

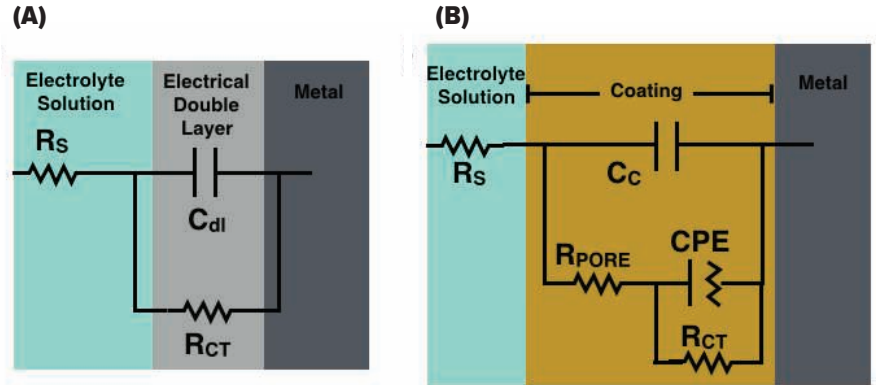

achieved a pseudo-plateau at –0.535 V, and further decreased to –0.650 V due to the active dissolution of the metallic substrate upon exposure to the electrolyte. Meanwhile, the E_{OCP} for the sample with the control waterborne paint (WBP) shifted to more noble potentials starting from –0.220 V and eventually stabilized at –0.515 V. The incorporation of either inhibitor resulted in a noticeable increase in the E_{OCP} immediately after electrolyte exposure, which can be attributed to an initial formation of a passive layer and/or corrosion products. After reaching a maximum of –0.11 V –0.08V, the E_{OCP} started to decrease and plateaued towards more positive E_{OCP} values as compared to the control WBP-coated and bare carbon steel samples. For paints incorporating the neutralized, aqueous solution of H570, the increase in E_{OCP} values is observed as follows: WBP (5% H570) = WBP (2% H570) > WBP (1% H570) > WBP (0.5% H570) > WBP > bare CS. Adding increasing amounts of H570 up to 2% concentration resulted in increased E_{OCP} values and improved corrosion inhibition properties, as shown in *Figure 2A*. The H570 concentrations above 5% resulted in more negative E_{OCP}. Therefore, 5% loading of H570 was identified as optimal loading concentration for the acrylic waterborne paint system. The similar inhibitor loading and E_{OCP} dependency was observed for paints incorporating the neutralized, aqueous solution of H650 inhibitor shown in *Figure 2B*. In this case, the E_{OCP} reaches a maximum of –0.37 V at 1% loading of H650, after one hour immersion in 5% aqueous NaCl solution.

Electrochemical Impedance Spectroscopy

In addition to E_{OCP} measurements, bare and paint-coated carbon steel samples were also analyzed using EIS. This is a key technique used in corrosion testing that provides accelerated corrosion data including information on coating degradation and ongoing corrosion on the metal surface based on the charge-transfer resistance (R_{CT}). The EIS technique can capture information such as the absolute impedance of the coating after the exposure to the corroding environment, thus probing for the corrosion inhibiting property of the coating. The high performance organic coatings provide corrosion protection by forming barriers that slow down the migration of electrolytes to the metal substrate. Therefore, monitoring the impedance of a particular coating can be used as a good and early predictor of a coating's performance in long-term salt spray studies.[5] Moreover, EIS is also used to probe for an equivalent circuit model wherein the polarization resistance and the capacitance of the coating can be quantified.

In the study, EIS measurements were performed after pre-corroding the samples in aqueous 5% NaCl solution for one hour. *Figure 3* presents the resulting Nyquist and impedance modulus-Bode plots for the bare carbon steel and the WBP coating with increasing concentrations of the H570 inhibitor. It can be seen that the diameter of the semi-circular Nyquist plots and the impedance modulus are increasing steadily as the inhibitor concentration increases. This behavior suggests increasing corrosion protection efficiency as more inhibitor is incorporated into the coating. In addition, it is also important to note that the bare carbon steel contains a single time constant due to the semicircular feature of the Nyquist plot. In the mid-frequency range, the Bode plot of the bare sample also contains a region wherein the curve is linear with a negative slope, which also complements this observation. On the other hand, the EIS plots of the coated samples contain two time constants: one at a high frequencies (more evident in the Bode plot) and another at a mid-frequency values. Monitoring the number of time constants in the EIS plots is considered when designing the equivalent circuit that best quantifies the behavior of the coatings.

Observing the time constants, the equivalent circuit models were then fitted onto the EIS plots recorded. *Figure 4* overlays the equivalent circuits used to characterize the behavior of the bare carbon steel and the coated steel samples onto schematic illustrations of the samples. *Figure 4A* illustrates a simplified Randles circuit, which is a common model for a corroding metal. It takes into account the resistance of the solution R_S, charge-transfer resistance R_{CT}, and the capacitive electrical double layer C_{DL}. The solution resistance, also known as the uncompensated resistance, is the resistance measured between the working and reference electrodes. The C_{DL} originates from the buildup of electrolytes on the metal surface. The R_{CT}, which is the most relevant factor to corrosion protection, takes into account the metallic oxidation or corrosion in equilibrium. On the other hand, *Figure 4B* is a modified electrical equivalent circuit model used to describe a metal with a porous coating and considers two main interfaces: the coating/electrolyte and coating/metal interfaces.[6] The capacitance C_C and pore resistance R_{PORE} of the coating and a constant phase element *CPE* are considered in this circuit to accurately depict the two interfaces. The *CPE,* known as an imperfect capacitor, was chosen

to replace the typical electrical double layer capacitance to achieve a much better simulation of the experimental data. Its value can be determined using equation (1) wherein *P* is the magnitude and *n* is an error factor.

$$CPE_{dl} = P^{1/n} R_{CT}^{(1-n)/n} \qquad (1)$$

After fitting the EIS data of the bare carbon steel into a simplified Randles circuit, it was determined that the solution resistance, double layer capacitance and charge-transfer resistance values equal to 7.62 Ω, 2.92 × 10^{-4} F, and 1.52 × 10^{3} Ω respectively. *Table 3* presents individual values of all elements of the equivalent circuit model for the paint-coated metal. The increase in the C_c is observed as the inhibitor concentration is increased. The C_c is defined by equation (2) in which ε is the dielectric constant of the coating, ε_o is the permittivity of free space with a constant value of 8.85 × 10^{-14} F/cm, *A* is the exposed area, and t is the thickness of a coating layer. Since the coating thickness and area are relatively the same, the dielectric constant or the insulating nature of the

TABLE 3—Individual Circuit Values from the EIS Data of the H570-Paint Coated Carbon Steel Samples after Immersion in 5% NaCl for One Hour

SAMPLE	R_S	C_C (F)	R_{PORE}	*P* of CPE	*n* of CPE	R_{CT}	%CPE
WBP	140.92	6.9493E-09	316.95	0.00017145	0.74644	9224.6	84%
WBP (0.5% H570)	67.532	1.3863E-08	100.09	0.000105	0.83665	11337	87%
WBP (1% H570)	85.282	1.4956E-08	116.63	8.107E-05	0.84026	16796	91%
WBP (2% H570)	121.34	1.5786E-08	169.13	4.9948E-05	0.72815	43900	97%
WBP (5% H570)	123.3	2.1014E-08	181.38	2.5274E-05	0.66223	1.0041E05	98%

TABLE 4—Individual Circuit Values from the EIS Data of the Bare and H570-Paint Coated Carbon Steel Samples after Immersion in 5% NaCl for One Hour

SAMPLE	R_S	C_C (F)	R_{PORE}	*P* of CPE	*n* of CPE	R_{CT}	%CPE
WBP	140.92	6.9493E-09	316.95	0.00017145	0.74644	9224.6	84%
WBP (0.5% H650)	151.06	6.6772E-09	319.05	0.00013265	0.77693	10146	85%
WBP (1% H650)	123.69	6.1379E-09	261.33	9.042E-05	0.83645	13325	89%

FIGURE 5—(A) Nyquist and (B) Bode impedance plots of the bare and H650-paint coated carbon steel samples after immersion in 5% NaCl for one hour.

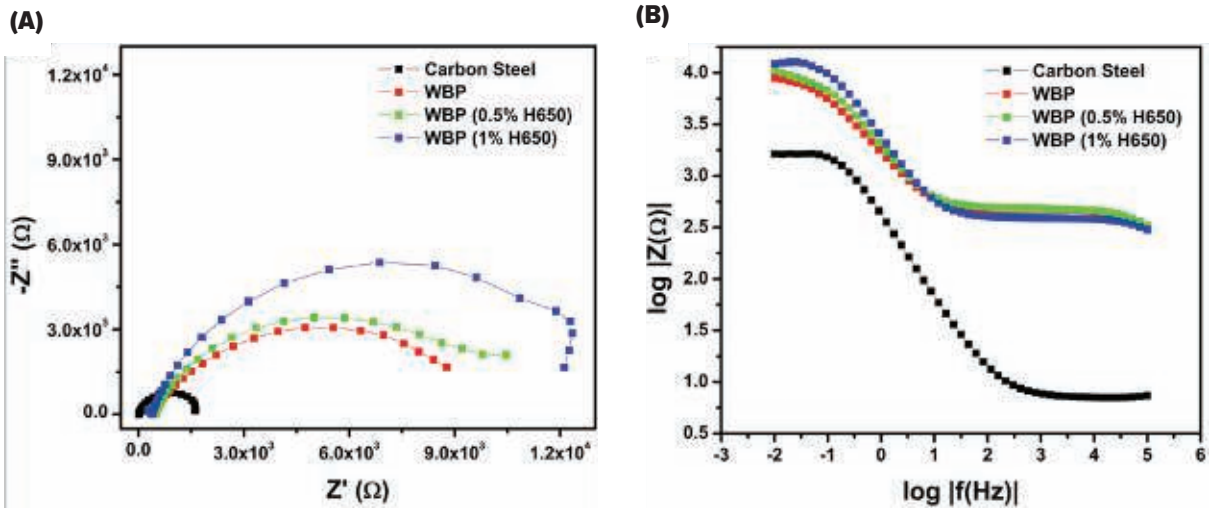

FIGURE 6—Tapping-mode AFM images of the (A) uncoated and (B) WBP-coated carbon steel samples.

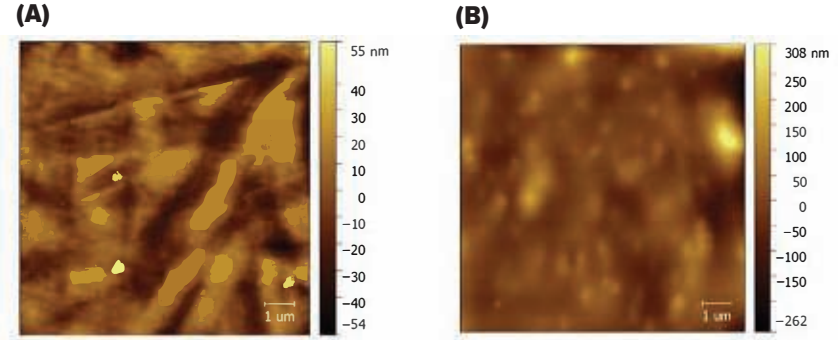

FIGURE 7—SEM images of the carbon steel samples coated with (A) WBP), (B) WBP with 5% H570, and (C) WBP with 1% H650.

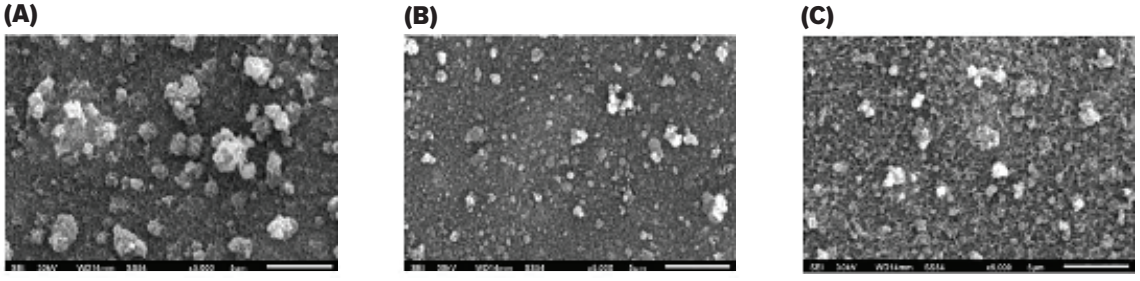

coating is increasing as larger amounts of corrosion inhibitors are added.

$$C_C = \frac{\varepsilon \times \varepsilon_o \times A}{t} \qquad (2)$$

In addition to the coating capacitance, the R_{CT} of the paint-coated samples also exhibited the similar increasing trend as a function of inhibitor concentration. From an R_{CT} of 9.22×10^3 Ω of the bare carbon steel, the charge transfer resistance reached a maximum of 1.00×10^5 Ω at 5% H570 inhibitor concentration. The corrosion protection efficiency can be calculated using equation (3). The determined R_{CT} values translated to protection efficiencies from 87% at 0.5% to 98% at 5% inhibitor concentration.

Figure 5 shows the Nyquist and Bode impedance plots of the paint coated-samples with the H650. As shown, the diameter of the semicircle Nyquist plots is increasing with inhibitor concentration up to 1%. The absolute impedance of a coating film is increasing accordingly. Similar to the performance of the coatings with H570, the paint-coated samples exhibited two time constants in the EIS plots. One is present at 10^4–10^5 Hz and the other lies between 10^{-1}–10^2 Hz. The same equivalent circuit model in *Figure 4B* is used to fit the experimental EIS data and extract the C_c and R_{CT} values.

Similar to the performance of the H570 inhibitor, paint coatings with the increasing amounts of H650 exhibited an increase in the R_{CT} values up to 1% of H650 inhibitor concentration. From the 9.22×10^3 Ω R_{CT} values of the control paint system, the charge-transfer resistance values increased to 1.01×10^4 Ω at 0.5% H650 and 1.33×10^4 Ω at 1 % H650 *(Table 4)*. These values translated to corrosion protection efficiencies of 85% and 89% for 0.5 and 1% H650 respectively. Higher inhibitor concentrations were analyzed but the corrosion inhibition started decreasing after 2%, 5%, and 10% inhibitor were added. These coatings, however, did not demonstrate a clear trend in the capacitance of the coatings.

$$\%\ \textbf{Corrosion Protection Efficiency} = \frac{R_{CT,o} - R_{CT}}{R_{CT,o}} \mathbf{X}\ 100\% \qquad (3)$$

Immersion Test

The surface morphology of the bare carbon steel sample and the freshly prepared paint-coated samples were imaged using AFM in tapping mode. As observed in *Figure 6A*, the metal surface contained ridges and grooves, which resulted from the sanding process during the surface preparation procedure. *Figure 6B* presents the AFM image of the control paint-coated substrates whose surface is significantly smoother than the uncoated samples. The control paint, however, contains various particle agglomerates embedded along the surface. Introducing either H570 or H650 inhibitors into these coatings resulted in similar surface morphological features.

These smooth control paint coated surfaces (WBP) deteriorated quickly within initial 24-h immersion in 5% aqueous NaCl solution. For comparison, coatings containing corrosion inhibitors with the best corrosion inhibition performance as determined according to the EIS results were immersed in 5% aqueous NaCl solution for 24 h as well to

FIGURE 8—Results of immersion testing in 5% NaCl for three weeks. (A) Digital images, (B) ATR-IR, and (C) Raman spectra of the uncoated and coated samples. (D) Adjusted Raman spectra highlighting the peaks of magnetite and TiO_2.

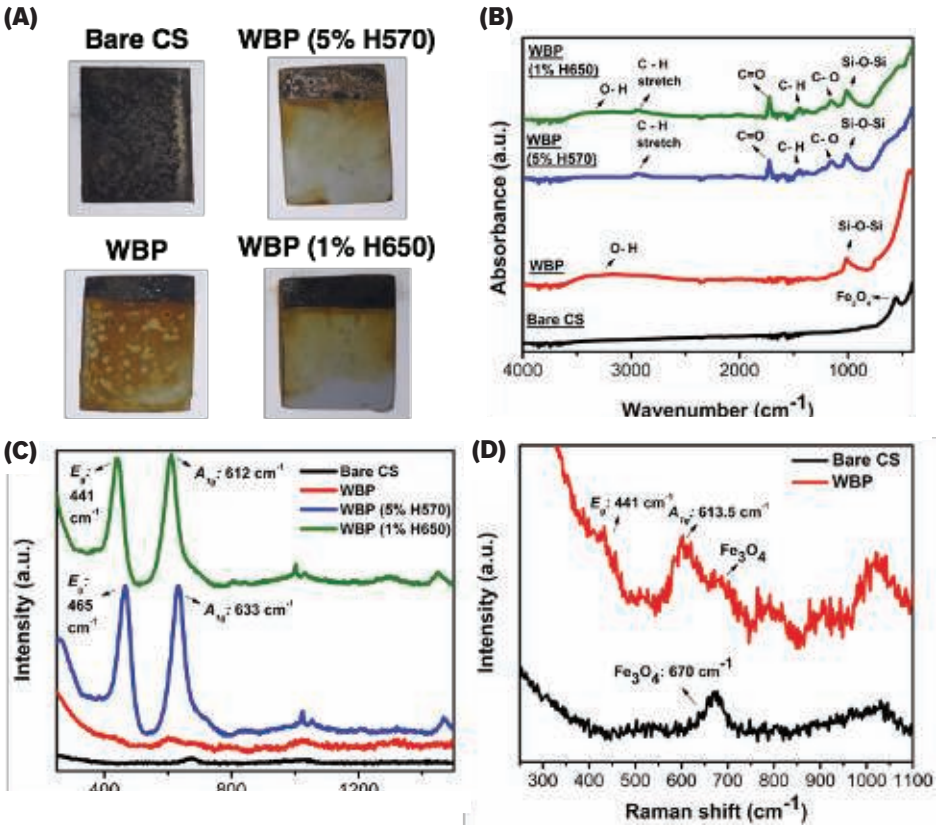

confirm the corrosion inhibitive properties exhibited in the electrochemical corrosion tests. *Figure 7* presents the scanning electron microscopy (SEM) images of the resulting surfaces of the samples coated with control paint, 5% H570, and 1% H650. The SEM examination of the surface morphology revealed that corrosion process resulted in the formations of the huge particle aggregates and blisters in the control paint system. This surface deterioration was observed to a certain extent for the WBP (1% H650) but with much smaller aggregates. Among these systems, WBP (5% H570) *(Figure 7B)* demonstrated the best corrosion protection since the resulting surface was much more homogenous and the corrosion byproducts (particle aggregates) were the smallest, which is in agreement with the EIS data obtained.

The prolonged immersion of the samples in the 5% aqueous NaCl solution was continued up to three weeks in order to investigate the long-term performance of the inhibitors. Attenuated total reflectance-infrared spectroscopy (ATR-IR) and Raman spectroscopy were used to gain better insight on the corrosion-related changes observed on the surface of the coated films. *Figure 8A* contains the digital images of the resulting samples after three-week exposure to the 5% aqueous NaCl solution. The black iron oxide rust, which is typically attributed to magnetite (Fe_3O_4), has covered the uncoated carbon steel samples. The control WBP-coated sample has almost completely discolored with various blistering and delaminated areas. Meanwhile, the paint coatings with both tested inhibitors showed intact original gray color, with no signs of blistering or deterioration in the paint film, which is in agreement with the electrochemical corrosion testing and SEM results. ATR-IR and Raman spectroscopy provide additional information on the corrosion products and the degradation of waterborne paint coating after three week immersion. As expected,

the coatings with inhibitors exhibited the signature peaks of a typical acrylic based paint formulation which include C=O at 1725 cm^{-1}, C–O at 1155 cm^{-1}, broad O–H peak at 3200–3600 cm^{-1}, C–H stretch between 2800–3000 cm^{-1} *(Figure 8B)*. Moreover, the out-of plane symmetric Si–O–Si peak was detected at 1011 cm^{-1}, which is attributed to the presence of talc ($Mg_3Si_4O_{10}(OH)_2$) in the paint coating. It is noticeable that most of these peaks have diminished from the IR spectra of the corroded sample coated with the control WBP. Only the O–H and Si–O–Si peaks remain, which suggests that progressive degradation of the coating in the corrosive environment. In addition, *Figure 8B* shows the IR spectra of the corroded uncoated carbon steel wherein a strong peak at 557.4 cm^{-1} corresponding to magnetite was detected.[6] The formation of the magnetite corrosion product was also detected as a strong peak at 670 cm^{-1} in the Raman spectral results in *Figures 8C* and *8D* due to the A_{1g} mode.[6,7] Similar to the trend of the IR spectroscopy, signature Raman peaks of the paint cannot be detected in the control WBP sample suggesting paint degradation. Typically, the Raman spectra of freshly prepared WBP possess the E_g and A_{1g} modes of titanium dioxide (TiO_2) at 448 cm^{-1} and 612 cm^{-1} respectively[8]. As seen in *Figure 8C,* these peaks were observed for WBP (5% H570) and WBP (1% H650). In *Figure 8D,* however, the TiO_2 peaks have significantly decreased. Furthermore, a Raman signal at 670 cm^{-1} also emerged due to the magnetite corrosion products on the sample. Hence, infrared and Raman spectroscopic techniques complement electrochemical corrosion testing results in observing the anticorrosion properties of the H570 and H650 inhibitors for waterborne paint coatings.

CONCLUSIONS

This study demonstrated the anticorrosive properties of a waterborne acrylic coating containing two organic corrosion inhibitors: H570 and H650. The open circuit potential measurements indicate the formation of a passive layer of corrosion products initially occurred for the corrosion inhibitor-containing paint-coated samples. Furthermore, open-circuit potentials for the formulation containing H570 and H650 shifted to the more noble values as the inhibitor concentration increased, suggesting improved anticorrosion properties of the paint film when compared to the control paint with no inhibitors. The anticorrosive activity imparted by organic corrosion inhibitors was further evidenced by electrochemical impedance spectroscopy measurements. The EIS demonstrated the increase in diameter values of the recorded Nyquist plot and absolute impedance values as a function of inhibitor concentration. By fitting an equivalent circuit model with two time constants, it was determined that maximum corrosion protection can be achieved by adding the inhibitor at 5% concentration for H570 and 1% for H650. In addition, the immersion measurements, which were monitored by scanning electron microscopy, reveal smaller blister diameters whenever these inhibitors were incorporated. Lastly, infrared and Raman spectroscopic techniques provided additional evidence to show that H570 and H650 corrosion inhibitors improved the long-term stability of the waterborne acrylic coating. Taking in account all the obtained data, it was shown that the addition of H570 at 5% was most beneficial in improving the tested waterborne acrylic coating's anticorrosive properties. ❊

ACKNOWLEDGMENTS

We acknowledge funding from the National Science Foundation, NSF STC-0423914 and CMMI NM 1333651. Technical support from Biolin Scientific, Inc., Agilent Technologies, and the Materials for Opto/Electronics Research and Education Center at Case Western Reserve University is also acknowledged.

References

1. Koch, G.H., Brongers, M.P.H., Thompson, N.G., Virmani, Y.P., and Payer, J.H., *Corrosion Cost and Preventive Strategies in the United States,* (2002). http://trid.trb.org/view.aspx?id=707382 (accessed October 6, 2014).
2. Koch, G., Varney, J., Thompson, N., Moghissi, O., Gould, M., and Payer, J., *International Measures of Prevention, Application, and Economics of Corrosion Technologies Study,* NACE International, 2016. http://impact.nace.org/documents/Nace-International-Report.pdf (accessed April 12, 2016).
3. Galliano, F. and Landolt, D., "Evaluation of Corrosion Protection Properties of Additives for Waterborne Epoxy Coatings on Steel," *Prog. Org. Coat., 44,* 217–225 (2002). doi:10.1016/S0300-9440(02)00016-4.
4. Thorn, A., Adams, A., Gichuhi, T., Novelli, W., and Sapp, M.A., "Improved Corrosion Control through Nontoxic Corrosion Inhibitor Synergies," *JCT CoatingsTech, 3,* 24–30 (2006).
5. Gichuhi, T., Balgeman, A., Prince, S., Wagner, C., O'Brien, S., and Adams, A., Employing Electrochemical Impedance in Predicting Corrosion Events," *JCT CoatingsTech, 8,* 32–38 (2011).
6. Pour-Ali, S., Dehghanian, C., and Kosari, A., "In situ Synthesis of Polyaniline–camphorsulfonate Particles in an Epoxy Matrix for Corrosion Protection of Mild Steel in NaCl Solution," 85 (2014) 204–214. doi:10.1016/j.corsci.2014.04.018.
7. Li, Y.-S., Church, J.S., and Woodhead, A.L., "Infrared and Raman spectroscopic studies on iron oxide magnetic nano-particles and their surface modifications," *J. Magn. Magn. Mater., 324*, 1543–1550 (2012). doi:10.1016/j.jmmm.2011.11.065.
8. Shebanova, O.N.,and Lazor, P., "Raman Spectroscopic study of magnetite (FeFe204): a New Assignment for the Vibrational Spectrum," *J. Solid State Chem., 174,* 424–430. (2003). doi:10.1016/S0022-4596(03)00294-9.
9. Balachandran, U. and Eror, N.G., "Raman Spectra of Titanium Dioxide," *J. Solid State Chem., 42,* 276–282 (1982). doi:10.1016/0022-4596(82)90006-8.

DR. B.D.B. TIU,* DR. S.B. TIU, J.R. WANG, and **PROF. R.C. ADVINCULA,*** Dept. of Macromolecular Science and Engineering, Case Western Reserve University, Cleveland, OH 44106, USA; Rigoberto.advincula@Case.edu;

Dr. S. Grubjesic, Dr. A.F. Toussaint, N. Kofira, and **Dr. T. Gichuhi,** ICL\ Advanced Additives, 1326 Summer St., Hammond, IN 46320.

*Dr. Tiu and Prof. Advincula are also associated with the Dept. of Biomedical Engineering, Case Western University.